Biomechanical analysis of controlled tibial blunt force trauma

Nicholas Dempsey, Felicity Maria Gilbert, Justyna Miszkiewicz and Marc F. Oxenham

College of Arts and social sciences, Archaeology and Anthropology, Australian National University, Canberra, Act, Australia

ABSTRACT

The analysis and interpretation of skeletal injuries caused by blunt force trauma (BFT) is often critical to reconstructing a victim's osteological profile. The manner in which bone fractures in response to BFT is a complex multiphasic process that involves interactions between mechanical force, skin and the musculo-skeletal system. To further improve our understanding of how bone fractures under mechanical force, this study investigated whether a quantifiable relationship was discernible between force and specific fracture outcomes (maximum fracture length, total fragment count and total anterior/posterior radiating fracture lines) and how anatomical factors influenced those outcomes. Fleshed sheep tibiae (*Ovis aries*, $n = 30$) were subjected to three conditions of force (90 N, 112 N and 135 N), ten tibiae at each force. Results indicate that a significant relationship exists between force and fracture length with respect to 90 N and 112 N force outcomes. No significant relationship was discernible between the level of force and the outcome variables of total fragment count and total anterior/posterior radiating fracture lines. These preliminary results suggest there is potential for further analysis of bone fracture behaviour under mechanical force with consideration to a broader suite of soft tissue and skeletal variables.

Introduction

Fractures encountered in forensic and human rights abuse cases are predominantly facilitated by blunt force trauma[1,2]. Broadly defined, blunt force trauma (BFT) refers to the non-penetrating physical injury from blunt objects during the application of mechanical forces over a wide area of impact[3–5]. The manner in which soft and skeletal tissues respond, materially and mechanically by absorbing and dissipating energy from an impact, influences how damage will manifest[6,7].

Within forensic anthropology, practical research into the mechanisms of bone fracturing is limited[8,9] and has predominantly been anecdotal and/or case study based[10]. Several studies have significantly contributed to understanding BFT in forensic anthropological contexts, by detailing differences in how fractures occur in ante/peri/post-mortem contexts, how fractures are classified, and the framework in which trauma studies can be further developed4,11,12.

Notwithstanding the limited amount of previous work, the impact of trauma to the musculo-skeletal system, broadly, has received minimal attention in the literature. To our knowledge, with the exception of Cohen et al.'s work[7], no forensic anthropological research into BFT has acknowledged or experimented with the effects of soft tissue on fracturing outcomes. This study incorporates soft tissue influences on fracture outcomes into the broader BFT equation. Given the relatively poorly understood mechanisms associated with BFT[13], research in this area will benefit medico-legal investigations in analysing how anatomical and biomechanical variables affect fracture outcomes.

The aim of this study is to determine whether a quantifiable relationship is discernible between force and the specific fracture outcomes of maximum fracture length, total fragment count, and total anterior/posterior radiating fracture lines and how anatomical factors may influence these outcomes. Biomechanical experiments were conducted using (n = 30) fleshed sheep tibiae (*Ovis aries*) where three conditions of force (90 N, 112 N and 135 N), consisting of (n = 10) specimens within each condition, were subjected to single controlled mechanical impacts to explore fracture outcomes. An evidence-based approach to the investigation of the relationship between force and trauma can contribute to minimizing subjective interpretation pertaining to the circumstances of traumatic impacts[14] and thus contributing to the investigation of trauma in a forensic context[15].

Materials and methods

Thirty fleshed domestic sheep (*Ovis aires*) tibiae, aged between 6–8 months, were subjected to three force conditions (n = 10 for each condition of 90 N, 112 N and 135 N). Force was generated by a gravitational accelerated mass (GAM) free falling into an impactor, causing three-point bending (Figure 1) and fracturing the tibiae.

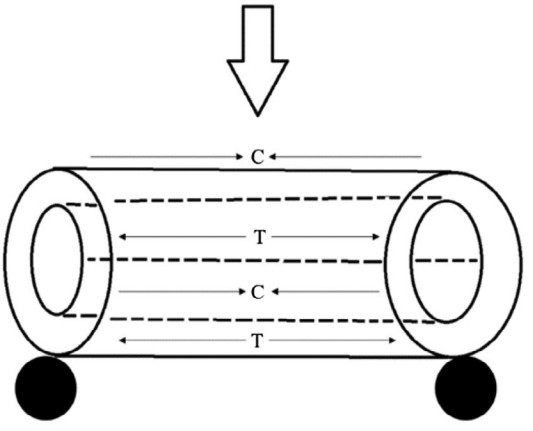

Figure 1. Basic conditions present during a three-point bend causing failure. the arrow (impacting the anterior aspect) is the transverse loading (the impact) direction. During three-point bending it causes the osteons in compression (c) to be crushed, while in tension (t), it pulls the atomic structure apart. the line through the centre (denoting the diaphyseal shaft) is the centroid and it is the three-point bending away from this line that causes the conditions for bone to fracture as conducted in these experiments. the black circles at the proximal and distal ends signify the areas where they were fastened in the impact jig.

Determination of force values

Pre-experimental tests on sheep tibiae, produced results that allowed the determination of appropriate upper and lower fracture thresholds. Four tests were conducted at 80 N which resulted in incomplete fracturing in each instance (green stick in morphology). Adjusting the threshold to 90 N produced complete fractures in four further trials, therefore setting the lower threshold. Four tests were conducted at 185 N and then another four tests at 150 N, all resulting in pulverization of the test tibiae. Finally, four trials were conducted at 135 N which provided significant damage of the tibial diaphysis, but without pulverization, which satisfied the research criteria of controlling for bone fractures over a range of three conditions. The value of 112 N, was determined by default, as it was the middle value between 90 N and 135 N. Force at impact was calculated by basic Newtonian physics:

$$F = m * h * g2$$

where the mass (m) of the GAM is 9.2 kg, the earth's gravitational constant is 9.81 m/s^2 (g), and the height of the drop tower (h), F is the energy prior to impact, which in the case of the experiments is between 90 N and 135 N. Table 1 provides the heights from which the forces were delivered and the corresponding force at time of impact.

Specimen description

It has been suggested that the more reliable model for assessing human fracturing has been the use of pig (*Sus scrofa domesticus*) models[16]. However, pig tibiae were not viable in these experiments as the lower limbs contain large amounts of soft tissue (e.g. *gastrocnemius* muscle) that would have prevented three-point bending during the impacts. Therefore, fleshed sheep (*Ovis ares*) were used due to their lower soft tissue levels. Fleshed specimens were employed to better model skeletal responses to blunt force trauma. The tissue depth along the tibial ridge (medial to the *tibialis anterior*), makes the tibial shaft highly susceptible to fracturing, providing a reliable medium for experimentation[17] and reasonable analogue for humans.

The specimens were purchased and collected fresh on the day of slaughter from a local butcher who cut them between the knee and ankle joint to retain their anatomical viability for the experiments. Specimens were tested at ambient temperature.

To allow for independent sample validity, the sample was randomized. This was to mitigate possible clustering effects in the statistical analysis. Soft tissues were tested for consistency on all specimens by tissue depth and ANOVAs were performed to confirm that no statistical differences existed.

Impact rig and specimen preparation

The delivery system used to apply force to the sheep specimens was a guided impact tower (Figure 2) that consisted of the delivery tube, impact area guide and impact jig for positioning the specimens. The purpose of this configuration was to prevent the impactor slipping off the specimen during impact, causing rotational behaviour in the specimen that could cause spiral/oblique fractures, which were not desirable for this experiment[4,18,19]. This impact rig was influenced by Desmoulin and Anderson[20], who used a similar rig for researching

Table 1. impact rig heights and corresponding impact forces.

Impactor height (m)	Time at impact (s)	Impact force (N)

1.00	0.45	90
1.25	0.51	112
1.50	0.55	135

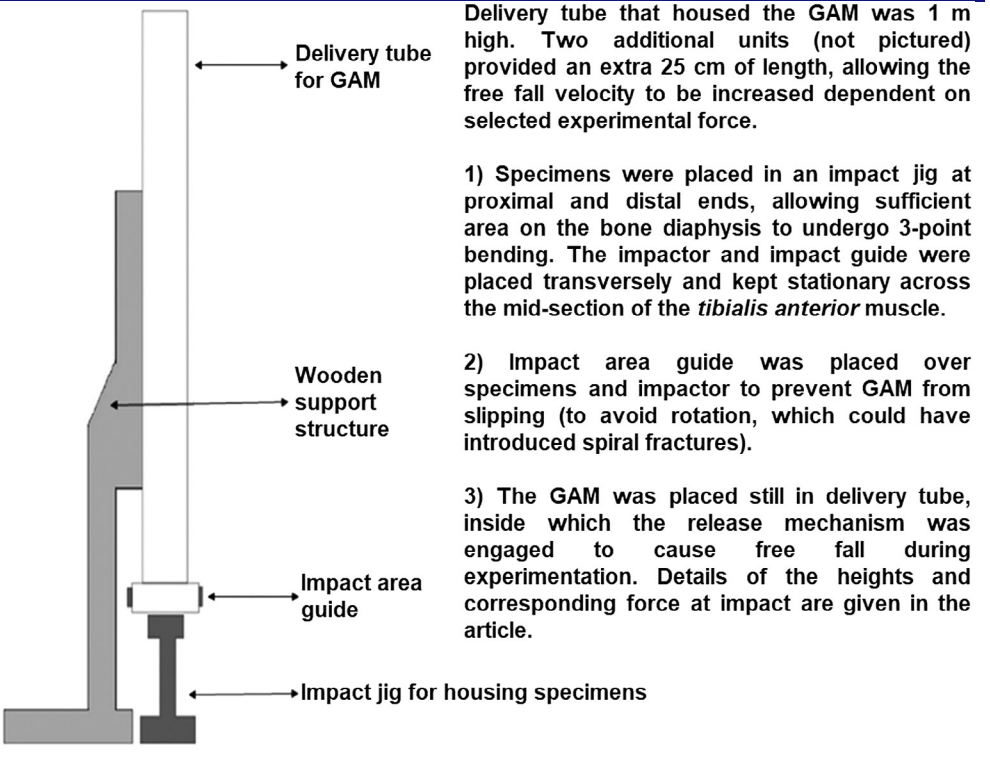

Figure 2. impact rig schematic.

contusion mechanics in human tissue. Placing the specimens in this configuration allowed for controlled, consistent replication of the 30 experiments across the three conditions.

Recording of fracture data

Maximum fracture length was measured using digital calipers (mm). Total fragment count was determined by counting the total bone fragments from each impact. Total anterior/posterior radiating fracture lines were counted by traversing the crack lines from the anterior and posterior surfaces where the radiating fractures originate from until their place of termination.

Statistical analysis of experimental data

The statistical analysis of the data was conducted using IBM Statistical Package for Social Science (SPSS) version 22. Univariate analyses of variance (ANOVA) were used to (1) analyse all the tibial characteristics in order to

determine whether any anatomical aspects varied that could have affected fracture outcomes and (2) analyse the relationship between force and the fracture outcomes of maximum fracture length, total fragment count and total anterior/posterior radiating fracture lines. Univariate analysis of variance is a useful statistical method in biomechanical analysis of fracturing, as it defines the relationship between the probability of an injury (fractures in this context) and a particular parameter (mechanical load). Post-hoc analysis using Tukey's HSD was used to analyse the differences between the forces regarding fracture outcomes if a significant value was obtained from the ANOVA tests.

Results

Qualitative outcomes

Out of the three conditions of force, fracture lengths from 90 N to 112 N showed a significant mean increase of 15.3 mm to 42.1 mm. From 112 N to 135 N, the mean fracture length only increased from 42.1 to 46.2 mm. Specimens subjected to the condition of 90 N did not generally present comminuted fractures with the majority being transverse. Fracture lengths were easily discernible and could be measured on the diaphysis. These predominantly short fractures measured between 7 to 13 mm and mainly radiated anteriorly from the fracture site.

Specimens subjected to the condition of 112 N were more definably damaged than at 90 N. The fracture morphology consisted of predominantly large fracture lines, radiating longitudinally along the anterior aspect of the tibial diaphysis. Complex multi-fragmentation in one case and one oblique fracture in another specimen were exceptions. Similar to 90 N, the predominant fracture lines were easily discernible on the diaphysis and featured relatively wider diaphyseal fractures in some specimens. The impact area where the fractures originated was generally more damaged on the anterior than the posterior surface. What differentiated the condition of 112 N from 90 N was that radiating lines were definable on the diaphysis (Figure 3), fractures were more pronounced and displayed a fracture typology of incomplete wedges.

There was definably more damage at 135 N compared with the other two force conditions. The fracture morphology was predominantly complex comminuted fractures that were heavily fragmented, as seen in Figure 3. Exceptions included a transverse fracture in one case and an oblique fracture in another. In some specimens, fracture typology manifested

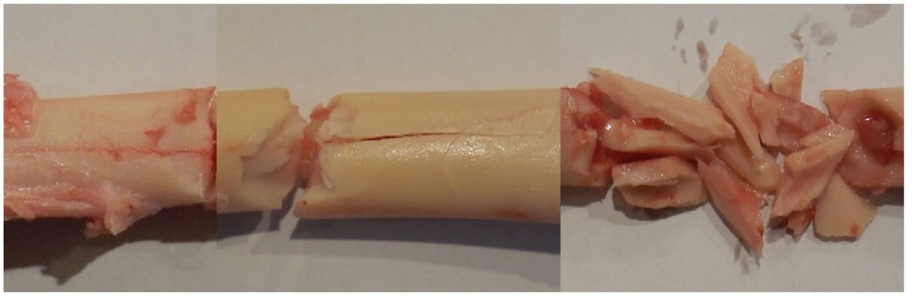

Figure 3. common fracture morphology of all three conditions of force, from left to right: 90 n, 112 n and 135 n. All post-impact tibiae are shown from the anterior aspect.

as complete butterfly fragments. What also differentiated 90 N and 112 N from 135 N, was the lack of definable radiating lines on the diaphysis in most specimens.

Quantitative outcomes

ANOVAs were performed on all anatomical variables (skeletal and soft tissue characteristics of the tibiae) to assess any differences in tibial characteristics across any of the three force conditions (Table 2). With the exception of anterior cortical bone thickness, there were no significant differences in tibial characteristics. The only fracture outcome that statistically significantly interacted with force was maximum fracture length (Table 3). Tukey HSD *post hoc* test indicated that fracture length (90 N) < fracture length (112 N) ($p < 0.000$), with fracture length (112 N) = fracture length (135 N) ($p = 0.6713$).

Discussion

Relationship between force and fracture length

There is a significant biomechanical relationship between force and fracture length, which indicates an increase in force is associated with an increase in fracturing (as measured by maximum fracture length). However, this relationship is not straightforward, and it would be difficult to predict force from fracture length alone using this model. What the results suggest is that differences in fracture outcomes will be a function of force, rather than underlying anatomical factors characterizing these tibiae.

Fracture length does not appear to vary when force increases from 112 to 135 N. The pre-trial experiments found that bone is pulverized at 150 N+, thus indicating that a plateau is reached at approximately 112 N, which remains relatively stable until approximately 150 N, after which bone responds in a

catastrophic manner. To further test the plateau model, more **Table 2.** Descriptive statistics of tibial characteristics, including AnoVAs.

	90 N (n = 10)		112 N (n = 10)		135 N (n = 10)			
Variable	Mean	STD. Dev.	Mean	STD. Dev.	Mean	STD. Dev.	F	P
Maximum tibial length	224.2	6.31	225.4	6.58	222.9	10.39	0.405	0.671
fleshed mid shaft circumference	120.4	7.33	127.1	6.40	134.1	11.60	1.69	0.204
Anterior soft tissue depth	11.3	1.28	12.2	2.17	13.2	1.76	3.18	0.060
Posterior soft tissue depth	16.4	2.39	16.4	2.29	16.9	2.78	1.57	0.226
Defleshed mid shaft circumference	58.4	1.50	59.2	2.48	60.2	1.68	2.12	0.140
Anterior cortical bone thickness	3.6	0.43	4.2	0.60	4.3	0.43	5.79	0.008*
Posterior cortical bone thickness	3.9	0.37	4.3	0.48	3.9	0.37	1.13	0.338
Medial cortical bone thickness	4.0	0.29	4.3	0.46	4.2	0.50	1.26	0.297
lateral cortical bone thickness	4.4	0.37	4.4	0.35	4.4	0.39	0.291	0.750

*refers to significant value < 0.5.

Table 3. Descriptive statistics of dependent variables contained within all force conditions, including AnoVAs.

	90 N (n = 10)		112 N (n = 10)		135 N (n = 10)			
Variable	Mean	STD. Dev.	Mean	STD. Dev.	Mean	STD. Dev.	F	P
Maximum fracture length	15.3	8.64	42.1	6.93	46.4	15.96	22.45	0.02*
total fragment count	2.8	2.25	3.4	3.50	5.2	4.33	3.38	0.49

total anterior radiating fracture lines	2.9	1.19	2.8	1.13	1.4	1.17	5.14	0.13
total posterior radiating fracture lines	2.5	2.7	2.5	1.58	1.6	2.0	0.57	0.57

*refers to significant value < 0.5.

force treatments between 112 N and 135 N would be required to be included in the experimental design. Another possibility, also consistent with an asymptotic relationship between force and fracture length, is that the amount of force required to produce a given fracture length increases in a non-linear manner.

In pre-trial tests at 150 N+, pulverization was observed. When the limits of normal fracture behaviour are met (crushing/pulverization), material is accompanied by nonlinear, irreversible and irrecoverable processes[21], where reconstruction is not viable. The small increase in fracture length between 112 N and 135 N suggests that the mechanical force limits of the sheep tibiae were being approached and possibly breached on occasion. Despite the possibility that the force of 135 N may have been too excessive, the mean fracture length in this group was the greatest out of the three conditions. Even though there was no statistically significant increase in fracture length between 112 and 135 N, an increase in fracture length did occur.

Qualitatively, facture lengths in the 90 N condition were easily discernible and measurable on the diaphysis as they were not severely damaged, as seen in Figure 3. The predominant fracture line at 90 N radiated longitudinally on the anterior aspect of the diaphysis. Although the measured fracture line was faint, it is likely that the lower boundary force of 90 N did not cause enough damage to overtly mask fracture lines (and their maximum length) in the sample. There was a minimal amount of deflection in the fracture line, indicating that the force it was subjected to was at a relatively low velocity. A large level of force can cause noticeable branching and a complex fracture morphology as seen at 112 and 135 N[22], whereas in the 90 N condition, only single fracture lines formed because of the small force.

Fracture lengths in the 112 N condition, when compared with the 90 N condition, were noticeably more defined in appearance, as seen in Figure 3. The fracture length was also larger than those associated with 90 N, radiating

longitudinally along the anterior aspect of the tibial diaphysis. Whereas at 90 N the fracture length did not deflect (i.e. branching of multiple fracture lines from a main fracture line), at 112 N deflection was demonstrated in the main fracture lengths recorded. This deflection relates to the increase of force and is indicative of increased stress on the diaphysis. High rates of stress in bone will cause radiating lines to deflect the forces applied and mitigate damage, a phenomenon known as fracture toughness[23,24].

Specimens subjected to the condition of 135 N were more definably damaged than both 90 N and 112 N mainly due to the more complex fracture morphology at this level of force. Most of the fractures in the 135 N treatment were multi-fragmented, making the measurement of fracture length difficult. Reconstructing the predominant fracture line (for measurement) at 135 N, was difficult due to the damage sustained on the diaphysis during the experiments, as seen in Figure 3. Due to this issue, some potential error in measuring total fracture length in the 135 N tibiae may have occurred.

From the whole sample, the largest fracture length was predominantly transverse in morphology. This specimen was subjected to 135 N with a fracture length of 83.07 mm, but it was not multi-fragmented and the diaphysis was intact. Although radiating fracture lines were predominant on the posterior aspect, the main fracture length traversed longitudinally along the anterior aspect. However, it appears that this was an anomalous specimen as, mechanically speaking, such a large fracture length should have caused multi-fragmentation, especially when compared with the others in the sample subjected to 135 N.

This case presented a pronounced fracture length without being affected by the complex fracture morphology that was present in the 135 N condition. This may be the result of the bone's ability to resist fracturing, known as fracture toughness[23,24]. Fracture toughness of material is determined by the ability of its microstructure to dissipate mechanical forces without propagation of a crack line[25]. This can occur due to different mechanisms such as viscoelastic or plastic flow, the formation of non-connected micro-cracks, crack ligament bridging and crack deflection[25,26]. As it is predominantly cortical bone that is damaged in these experiments, cement lines within the cortical matrix can reveal fracture lines forming transversely in the bone, demonstrating crack deflection as it interacts with the underlying Haversian structures[27,28]

Although some specimens appeared pulverized, it appears that they were subjected to three-point bending during impact and were thus conducive to the mechanical conditions being analysed. This is confirmed by the observation that the fragments that comprised the diaphysis could be reconstructed. If normal loading conditions have been exceeded, then irreversible and irrecoverable processes prevent reconstruction of the bone/material[21].

Relationship between force and total fragment count

At 90 N, fragments mainly comprised small shards of bone that predominantly derived from the fracture site. Although the material properties of juvenile bone possess a greater capacity to limit fracture propagation[29], it was interesting to find that this feature was only observed at 90 N, indicating that the lower force was the mitigating factor. Some specimens did present butterfly-like fragments, however, this was atypical of 90 N.

At 112 N, fragments were more defined and were medium to large in size. Compared with 90 N, which consisted of small shards of bone, the fragments at 112 N could be recognized as parts of the tibial diaphysis. There were no shards of bone at 112 N. At 135 N, the overall size of fragments was smaller but the most obvious difference was the larger overall fragment count. In the lower forces it was easy to discern that the fragments were parts of the diaphysis, however, at 135 N their appearance of being part of the tibiae (especially if placed out of context) would be difficult to determine. Like 112 N, 135 N also had no bone shards from the fracture site.

The homeostatic processes that develop during osteogenic differentiation between individuals may contribute to the variation in the total fragment count regardless of the force condition[4,23]. For example, a specimen subjected to 135 N may have been predisposed (homeostatic differences between specimens) to such damage even at 90 N, revealing possible biological factors that could not be accounted for prior to experimentation. This further demonstrates the complexities of bone as a material and, unfortunately, reveals confounding factors in analysing the relationships between force and fracturing. While force is a factor in causing bone fragmentation, there are numerous biological, physical and anatomical variables that need to be accounted for in this process such as tissue depth, area of impact and muscle tension due to reflexive behaviours.

Relationship between force and total anterior/posterior radiating fracture lines

At 90 N, faint radiating fracture lines were more noticeable on the anterior than posterior aspect of the diaphysis. These radiating fracture lines propagated from the fracture site minimally along the diaphysis and did not significantly traverse longitudinally towards the distal and proximal aspects (which was noticeable at 112 N). Because fracturing is time-dependent (e.g. the higher velocity, the higher the probability of fracturing compared with a slower velocity), the increased contact time during the 90 N condition may explain why more radiating fractures were present.

At 112 N, radiating fracture lines appeared more noticeable anteriorly than posteriorly. The radiating fracture lines also appeared more defined on the diaphysis than at 90 N due to the increase in force. This, however, did not result in more fracture lines and overall, they decreased both anteriorly and posteriorly. Compared with 90 N, radiating fracture lines were more visible on the diaphysis, and the branching patterns indicated the higher level of force applied.

Although it appeared to consist of more damage, the 112 N group was less affected by radiating fracture lines both anteriorly and posteriorly compared with the 90 N condition. While there is a general correlation between force and bone fracturing[18], it is possible that material/mechanical factors that could not be accounted for, such as osteon density, bone mineral density and collagen density, influenced the relatively reduced number of radiating fracture lines at 112 N.

For 135 N, radiating fracture lines were non-existent as the area of impact was highly comminuted. Interestingly, even at the proximal and distal aspects of the impacted tibiae beyond the boundaries of the fracture site, no radiating lines were noticeable.

Conducting blunt force trauma experiments on non-living subjects is somewhat problematic, as potentially mitigating physiological reactions in a living subject are inactive in deceased subjects. The incorporation of soft tissue as a characteristic of the impacted sheep tibiae cannot fully emulate the trauma responses in a living subject. However, the use of soft tissue in these experiments presents an opportunity to explore questions of muscle-bone interactions during blunt force trauma[30].

During the experiments, there was no axial (compressive) loading on the superior and inferior aspects. This limitation was unavoidable due to a lack of appropriate materials and facilities to incorporate this condition. Instances of trauma to the lower extremities are multiaxial loaded[31,32]. Despite limitations, a positive correlation was found between force and maximum fracture length, demonstrating that there is a relationship that can be further explored with an improved methodology, different anatomical/biological variables and larger dataset.

Conclusions

While these experiments have demonstrated a significant correlation between increasing force and increasing fracture lengths, this relationship is complicated. The relationship between force and fracturing was only significant between 90 N to 112 N. The variables of total fragment count and radiating fracture lines were not clearly related to increases in force. Although

the relationship between force and fracturing was significant between 90 N to 112 N, this result is provisional until corroborated by further experiments. The notion that increases in force correspond to increased fracture damage (particularly total anterior/posterior radiating fracture lines) requires re-evaluation.

This study analysed bone fracturing as a multiphasic interaction from a perspective of the soft and skeletal anatomical structures involved. The novel inclusion of soft tissue anatomical factors in exploring fracturing was intrinsically valuable as it allowed an assessment into what conditions are required to construct robust analyses of fracture outcomes. Bone fractures caused by blunt force trauma cannot be analysed in isolation as fracturing is clearly influenced by interactions within the muscular-skeletal system as a whole. Although the soft tissue utilized in these experiments was not physiologically active, it still biomechanically influenced the fracture outcomes because of the muscle-bone interaction.

Understanding the relationship between forces, fracturing and how anatomical/biological factors influence this phenomena through the use of scientific analysis can remove the subjective interpretation of circumstances surrounding traumatic impacts[14]. The research reveals that this relationship is more complex than a simple dichotomy between fracturing and force. While further research is needed, the ability to correlate levels of force with fracture outcomes in a medico legal context has the potential to provide valuable information on the mechanisms (and perhaps intent and/or circumstances) associated with blunt force trauma events.

References

1. Mole CG, Heyns M, Cloete T. How hard is hard enough? An investigation of the force associated with lateral blunt force trauma to the porcine cranium. Leg Med. 2015;17(1):1–8. https://doi.org/10.1016/j.legalmed.2014.07.008.
2. Sulaiman NA, Osman K, Hamzah NH, Hamzah SPAA. Blunt force trauma to skull with various instruments. Mal j Path. 2014;36(1):33–39. https://doi.org/953bd9fecefe935e1cdfe11fae15b16e /1?pq-origsite=gscholar
3. Kranioti E. Forensic investigation of cranial injuries due to blunt force trauma: current best practice. Res Rep Forensic Med Sci. 2015;5(1):25–37. https://doi.org/10.2147/RRFMS.S70423.
4. Wedel VL, Galloway A. Broken bones: anthropological analysis of blunt force trauma. 2nd ed. Springfield (IL): Charles C. Thomas Ltd; 2014.
5. Byers SN. Introduction to forensic anthropology. 4th ed. Boston (MA): Prentice Hall; 2011.

6. Cohen H, Kugel C, May H, Medlej B, Stein D, Slon V, Brosh T, Hershkovitz I. The influence of impact direction and axial loading on the bone fracture pattern. Forensic Sci Int. 2017;277(1):197–206. doi:10.1016/j.forsciint.2017.05.015
7. Cohen H, Kugel C, May H, Medlej B, Stein D, Slon V, Brosh T, Hershkovitz I. The effect of impact tool geometry and soft material covering on long bone fracture patterns in children. Int J Legal Med. 2017;131(4):1011–1021. doi:10.1007/s00414-017-1532-7
8. Davidson, K, Davies, C, Randolph-Quinney, P Skeletal Trauma. In: Ferguson, EilidhSM, Ferguson, E, editors. Forensic anthropology: 2000 to 2010. Boca Raton (FL): CRC Press; 2011. p. 183–235.
9. Wheatley BP. Perimortem or postmortem bone fractures? An experimental study of fracture patterns in Deer Femora. Journal of Forensic Sciences. 2008;53(1):69–72. doi:10.1111/j.1556-4029.2008.00593.
10. Scheuer L, Black SM. Developmental juvenile osteology. San Diego (CA): Academic Press; 2000.
11. Berryman and Symes. Recognising gunshot and blunt cranial trauma through fracture interpretation. In: Reichs K, editor. Forensic osteology: advances in the identification of human remains. Springfield (IL): Charles C Thomas; 1998; p. 333–352.
12. Passalacqua, NV, Fenton, TW Developments in skeletal trauma: blunt-force trauma. In: Dirkmaat, DC, editors. A Companion to Forensic Anthropology. Chichester (UK): John Wiley & Sons, Ltd; 2012. p. 400–411.
13. Dirkmaat D, editor. A companion to forensic anthropology, Blackwell companions to anthropology. Malden (MA): Wiley-Blackwell; 2012.
14. Porta, DJ. Skeletal trauma analysis of the lower extremity. In: Rich, J, Dean, DE, Powers, RH, editors. Forensic medicine of the lower extremity: human identification and trauma analysis of the thigh, leg, and foot. Totowa (NJ): Humana Press; 2005. p. 253–277.
15. Gläser N, Kneubuehl BP, Zuber S, Axmann S, Ketterer T, Thali MJ, Bolliger SA. Biomechanical examination of blunt trauma due to baseball bat blows to the head. Journal of Forensic, Biomechanics. 2011;2(1):1–5. doi:10.4172/2090-2697.1000108.
16. An, YH, Friedman, RJ. Animal selection in orthopaedic research. In: An, YH, Friedman, RJ editors, Animal models in orthopaedic research. Boca Raton (FL): CRC Press; 1999. p. 39–59.
17. Koval KJ, Zuckerman JD. Handbook of fractures. 3rd ed. Philadelphia (PA): Lippincott Williams & Wilkins; 2006.
18. Cohen H, Kugel C, May H, Medlej B, Stein D, Slon V, Hershkovitz I, Brosh T. The impact velocity and bone fracture pattern: forensic perspective. Forensic Sci Int. 2016;266(1):54–62. doi:10.1016/j. forsciint.2016.04.035.

19. Sullivan CM. Child abuse and the legal system: the orthopaedic surgeon's role in diagnosis. Clin Orthop Relat Res. 2011;469(3):768–775.
20. Desmoulin GT, Anderson GS. Method to investigate contusion mechanics in living humans. Journal of Forensic Biomechanics. 2011;2(1):1–10. doi:10.4303/jfb/F100402
21. Ryu H, Saito F. Single particle crushing of nonmetallic inorganic brittle materials. Solid State Ionics. 1991;47(1-2):35–50. doi:10.1016/0167-2738(91)90177-D.
22. Behari J. Biophysical bone behaviour: principles and applications. Chichester (UK): John Wiley & Sons, Ltd; 2009.
23. Gdoutos EE. Fracture mechanics: an introduction. 2nd ed. Norwell (MA): Springer; 2005.
24. Nyman JS, Makowski AJ. The contribution of the extracellular matrix to the fracture resistance of bone. Curr Osteop Repo. 2012;10(2):169–177. doi:10.1007/s11914-012-0101-8
25. Fratzl P 2008. Bone fracture: when the cracks begin to show. Nature Materials. 2008; 7(8); 610–612. doi:10.1038/nmat2240.
26. Meyers MA, Chen PY. Biological materials science: biological materials, bioinspired materials, and biomaterials. New York (NY): Cambridge University Press; 2014.
27. Withers PJ. Fracture mechanics by three-dimensional crack-tip synchrotron X-ray microscopy. Phil. Trans. R. Soc. A. 2015;373(2036): 20130157–20130157. doi:10.1098/rsta.2013.0157.
28. Leng H, Wang X, Ross RD, Niebur GL, Roeder RK. Micro-computed tomography of fatigue microdamage in cortical bone using a barium sulfate contrast agent. J Mech Behav Biomed Mater. 2008;1(1):68–75. doi:10.1016/j.jmbbm.2007.06.002.
29. Ubelaker DH, Montaperto KM. Biomechanical and remodelling factors in the interpretation of fractures in juveniles. In: Ross AH, Abel SM, editors. The Juvenile skeleton in forensic abuse investigations. New York (NY): Humana Press; 2011; p. 33–48.
30. Graham AE, Xie SQ, Aw KC, Mukherjee S, Xu WL. Bone–muscle interaction of the fractured femur. J Orthop Res. 2008;26(8):1159–1165. doi:10.1002/jor.20611.
31. Funk JR, Rudd RW, Kerrigan JR, Crandall JR. The effect of tibial curvature and fibular loading on the tibia index. Traffic Injury Prevention. 2014;5(2):164–172. doi:10.1080/15389580490436069.
32. Galloway, A, Zephro, L Skeletal trauma analysis of the lower extremity'. In: Rich, J, Dean, DE, Powers, RH, editors. Forensic medicine of the lower extremity: human identification and trauma analysis of the thigh, leg, and foot. Totowa (NJ): Humana Press; 2005. p. 253–277.